

Implications of the Convergence of Language and Vision Model Geometries

Jiaang Li

University of Copenhagen

Yova Kementchedjheva

University of Copenhagen

Anders Søgaard

University of Copenhagen

Abstract

Large-scale pretrained language models (LMs) are said to “lack the ability to connect [their] utterances to the world” (Bender and Koller, 2020). If so, we would expect LM representations to be unrelated to representations in computer vision models. To investigate this, we present an empirical evaluation across three different LMs (BERT, GPT2, and OPT) and three computer vision models (VMs, including ResNet, SegFormer, and MAE). Our experiments show that LMs converge towards representations that are partially isomorphic to those of VMs, with dispersion, and polysemy both factoring into the alignability of vision and language spaces. We discuss the implications of this finding.

1 Introduction

The idea that computers are ‘all syntax, no semantics’ has a long history, which can be traced back to German 17th century philosopher Gottfried Wilhelm Leibniz,¹ but it was widely popularized by American philosopher John Searle. In 1980, Searle’s Chinese Room (Searle, 1980) quickly became one of modern philosophy’s most influential thought experiments. The Chinese Room is the idea of an interlocutor with no prior knowledge of a foreign language, who receives text messages in this language and follows a rule book to reply to the messages. The interlocutor is Searle’s caricature of artificial intelligence, and is obviously, Searle claims, not endowed with meaning or understanding, but merely acts on symbol manipulation.

In one of the most cited artificial intelligence papers of 2020, which also won the ACL 2020 Best Theme Paper Award, Emily Bender and Alexander Koller (Bender and Koller, 2020) presented a

¹Leibniz’s Mill Argument has been used to argue against the possibility of strong AI (Lodge and Bobro, 1998). The Mill Argument states that mental states cannot be reduced to physical states, so if human-level intelligence, including the ability to understand language, requires mental states, strong AI cannot exist.

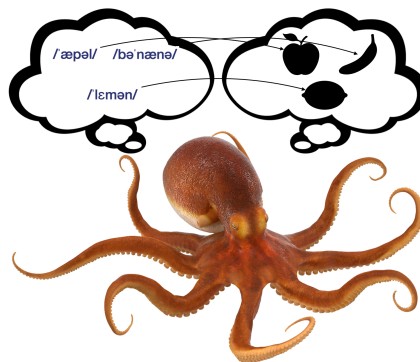


Figure 1: The Octopus of Bender and Koller (2020) mapping a word vector space into an image vector space.

modified version of Searle’s Chinese Room argument, the so-called *Octopus Argument*. In brief, they replace the rule-based interlocutor in Searle’s Chinese Room with an interlocutor that is ‘very good at detecting statistical patterns’, i.e., a better-than-GPT-3, hypothetical language model. They use the thought experiment to arrive at the same conclusion as Searle did: computers cannot acquire meaning from raw text.

Bender and Koller (2020) present us with the following scenario: Two humans A and B, each stuck on a deserted island, communicate regularly through an underwater cable. A statistical learner in the form of a hyper-intelligent octopus taps in on the cable communication, while unable to visit or observe the islands. After a period of learning to predict what A and B will say, the octopus cuts the cable and inserts himself, pretending to be B. Like Searle, Bender and Koller argue that the octopus, regardless of how good it becomes at imitating B, does not and never will truly understand the language of A. The octopus, a stand-in for a pretrained language model, will never learn the meaning, which they define as a mapping of expressions onto communicative intent about the world. They claim that:

The extent to which O can fool A depends on the task — that is, on what A is trying to talk about. A and B have spent a lot of time exchanging trivial notes about their daily lives to make the long island evenings more enjoyable. It seems possible that O would be able to produce new sentences of the kind B used to produce; essentially acting as a chatbot. This is because the utterances in such conversations have a primarily social function, and do not need to be grounded in the particulars of the interlocutors’ actual physical situation nor anything else specific about the real world. It is sufficient to produce text that is internally coherent.

Others have added nuance to this position, claiming that while LMs possibly do not learn referential semantics, they do learn inferential semantics (Sahlgren and Carlsson, 2021; Piantadosi and Hill, 2022). Our experiments below suggest that they learn more than that.

To highlight the role of reference – or grounding (Harnad, 2007) – Bender and Koller also present the following *more constrained* version of their thought experiment:

As a second example, imagine training an LM (again, of any type) on English text, again with no associated independent indications of speaker intent. The system is also given access to a very large collection of unlabeled photos, but without any connection between the text and the photos. For the text data, the training task is purely one of predicting form. For the image data, the training task could be anything, so long as it only involves the images. At test time, we present the model with inputs consisting of an utterance and a photograph, like *How many dogs in the picture are jumping?* or *Kim saw this picture and said “What a cute dog” What is cute?*

This second thought experiment highlights the importance of grounding word representations to representations of what they refer to. It also shows what their argument hinges on: If unsupervised or very weakly supervised alignment of language models and computer vision models is possible, their argument fails completely. The empirical

question then is whether such alignment of the two modalities is possible.

Bender and Koller deem language models unable to ‘connect their utterances to the world’ because they assume that their representations are unrelated to representations in computer vision models. If the two representations were structurally similar, however, it would take just a simple linear mapping to make proxy inferences about the world and to establish reference. As long as the representations of computer vision models are learned independently from the representations of language models, any structural similarities between the two should provide strong evidence that language models have at least some ability to connect to the world. In this paper, we show that such an alignment is possible.

Contributions We present a series of evaluations of the vector spaces induced by three families of language models and three computer vision models for a total of 12 language models and 14 computer vision models. We show that within each family, the larger the language models, the more their vector spaces become structurally similar to those of computer vision models. This enables easy retrieval of language representations of images (referential semantics). Retrieval precision depends on dispersion (visual and language) and polysemy, but consistently improves with language model size. We discuss the implications of the finding that language and computer vision models converge on similar geometries.

2 Methodology

Our experiments are designed to empirically test Bender and Koller’s second thought experiment. We therefore induce representations from vision and language models and evaluate the alignability of these representations. We further focus on the convergence of these similarities as model sizes increase (C and King, 2022). Below we introduce the pretrained models we use and the procedure for aligning their representations.

2.1 Pretrained Language and Vision Models

Language models We include 12 Transformer-based language models (LMs) in our experiments, representing three families of models: BERT (Devlin et al., 2019), GPT2 (Radford et al., 2019), and OPT (Zhang et al., 2022). Details of the models are listed in Table 1.

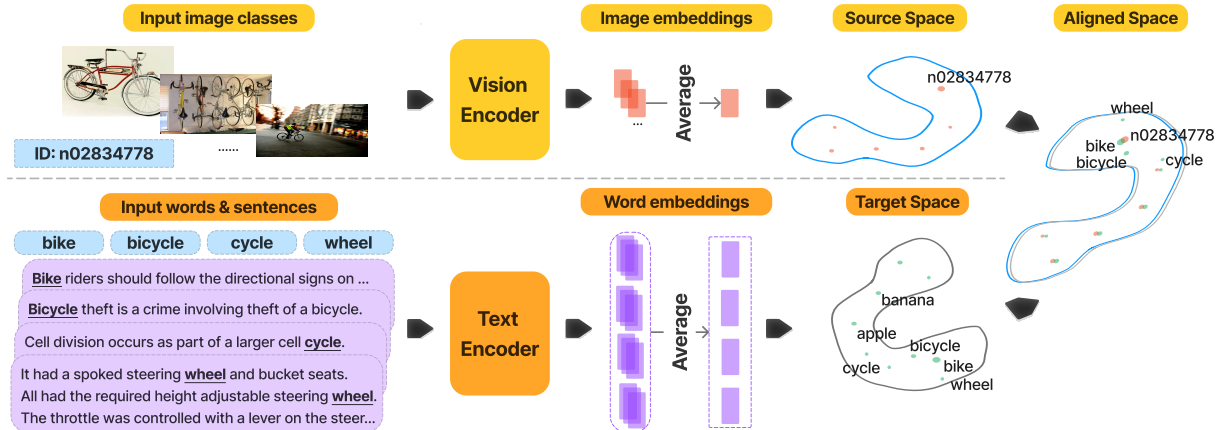


Figure 2: Experiments stages: During our experiments, words, sentences, and images are selected from the aliases list (wordlist and ImageNet-21k aliases), Wikipedia and ImageNet-21k, respectively. The source and target spaces are constructed by image and word embeddings which are encoded by specialized vision and language encoders.

BERT is a Transformer-based LM, which makes use of a multi-headed attention mechanism to selectively attend to different parts of the context when predicting masked tokens (in masked language modeling). Each Transformer layer combines this information in a quadratic pass over the input tokens. The input tokens are represented by combinations of token embeddings and position embeddings. It is designed to understand the context of a given text by processing the input in a bidirectional manner, which means that it can predict the masked words based on both the left and right context. We use five different sizes of BERT, including BERT_{BASE} and BERT_{LARGE}, which are pretrained on the BooksCorpus and English Wikipedia. The remaining BERT models included are pretrained with distilled from BERT_{LARGE} (Turc et al., 2019). All BERT models we use are uncased.

GPT2, one of the causal LMs based on decoder-only Transformer architecture, only takes on the left context to predict next tokens. It is capable of generating human-like text and can be finetuned for a wide range of natural language processing tasks such as text generation, summarization, and question answering. GPT2-type models are pretrained on the WebText dataset.

OPT is also a suit of decoder-only pretrained Transformer-based LMs like GPT2. It has demonstrated remarkable emergent capabilities, including the ability to generate text and perform zero- and few-shot learning tasks. We use OPT because it is much bigger than GPT2 and trained on more data. OPT-type models are pretrained on a union of the following five datasets: BookCorpus, CC-

LMs	Params	Datasets
BERT _{TINY}	4.4M	
BERT _{MINI}	11.3M	
BERT _{SMALL}	29.1M	BooksCorpus (Zhu et al., 2015);
BERT _{MEDIUM}	41.7M	English Wikipedia (Devlin et al., 2019)
BERT _{BASE}	110.1M	
BERT _{LARGE}	340M	
GPT2 _{BASE}	124M	
GPT2 _{LARGE}	774M	WebText (Radford et al., 2019)
GPT2 _{XL}	1542M	
OPT _{125M}	125M	BooksCorpus;
OPT _{6.7B}	6.7B	CC-Stories (Trinh and Le, 2018);
OPT _{30B}	30B	CCNewsV2 (Zhang et al., 2022);
		The Pile (Gao et al., 2021);
		Pushshift.io Reddit dataset
		(Baumgartner et al., 2020)

Table 1: The 12 language models used in our experiments. Appendix E Table 5 lists the links of LMs.

Stories, CCNewsV2², a subset of the Pile (Pile-CC, OpenWebText2, USPTO, Project Gutenberg, OpenSubtitles, Wikipedia, DM Mathematics, and HackerNews), and Pushshift.io Reddit dataset as processed by Roller et al. (2021).

Vision models We include 14 computer vision models (VMs) in our experiments, representing three families of models: SegFormer (Xie et al., 2021), MAE (He et al., 2022), and ResNet (He et al., 2016). Details of models are listed in Table 2.

SegFormer models consist of a Transformer-based encoder and a light-weight feed-forward decoder. They are pretrained on object classification data and finetuned on scene parsing data for scene segmentation and object classification.

²The English section of the CommonCrawl News dataset, which was used in RoBERTa (Liu et al., 2019), is updated in CCNewsV2.

VMs	Params	Datasets
SegFormer-B0	3.4M	
SegFormer-B1	13.1M	ADE20K
SegFormer-B2	24.2M	(Zhou et al., 2017)
SegFormer-B3	44.0M	ImageNet-1K
SegFormer-B4	60.8M	(Russakovsky et al., 2015)
SegFormer-B5	81.4M	
<hr/>		
MAE _{BASE}	86M	
MAE _{LARGE}	304M	ImageNet-1K
MAE _{HUGE}	632M	
<hr/>		
ResNet18	11.7M	
ResNet34	21.8M	
ResNet50	25.6M	ImageNet-1K
ResNet101	44.6M	
ResNet152	60.2M	

Table 2: The 14 computer vision models used in our experiments. Appendix E Table 6 lists the links of VMs.

We hypothesize that the reasoning necessary to perform segmentation in context promotes representations that are more similar to those of LMs, which also operate in a discrete space (a vocabulary). The SegFormer models we use are pretrained with ImageNet-1K and finetuned with ADE20K.

MAE models have a Transformer-based encoder-decoder architecture. They are trained to reconstruct masked patches in images, which is a fully unsupervised training objective, similar to masked language modeling. The encoder takes as input the unmasked image patches while a light-weight decoder reconstructs the original image from the latent representation of unmasked patches interleaved with mask tokens. The MAE models we use are pretrained on ImageNet-1K.

ResNet models consist of a bottle-neck convolutional neural networks with residual blocks as an encoder, followed by a classification head that makes predictions based on the encoded representation. They are pretrained on the ImageNet-1k dataset for the task of object classification.

For all three types of VMs, we only employ the encoder component as visual feature extractor.

2.2 Bimodal Data Compilation

We build a bimodal dictionary of image-text pairs based on the ImageNet-21k dataset (Russakovsky et al., 2015) to learn a mapping between two modalities. In ImageNet, a concept class is represented by multiple images and one or more names (which we refer to as aliases), many of which are multi-word expressions. The LMs included here were trained

on sentences and paragraphs of text, which means that applying them directly to words in isolation could result in unpredictable behavior. Instead, we obtain natural occurrences of these words together with the surrounding context (full sentence) from English Wikipedia.

We filter the data from ImageNet according to the following criteria: we keep classes with over 100 images available, we keep aliases that appear at least 5 times in Wikipedia, and classes with at least one alias left after the alias filtering. 11,338 classes meet these criteria and the final count of image-text pairs is 15,646 (since some classes have multiple aliases). The classes in this bimodal dictionary are split 70-15-15 for training, validation and testing. We perform five such splits at random and report averaged results.

2.3 Data Encoding and Cross-modal Alignment

The following procedure description is illustrated in Figure 2.

Image representations The visual representation of a concept is obtained by embedding up to 200 of the images available for the concept with a given VM and then averaging these representations. ResNet and SegFormer models generate a single vector per input image. When applying MAE models, we take the CLS token representation as the basis for every image.

Text representations The language representation of a concept is obtained by embedding an alias in up to 15 sentences from Wikipedia that contain the target word or phrase, averaging over the representations of the corresponding wordpieces, and then decontextualizing those resulting representations (Abdou et al., 2021).

Linear projection We use Procrustes analysis (Schönemann, 1966) to align the representations of computer vision models to those of language models, given a bimodal dictionary (Conneau et al., 2018). Procrustes analysis is a form of statistical shape analysis, done by matching corresponding points in the shapes and finding the transformation (translation, rotation, and scaling) that best aligns them. Procrustes analysis has been used in many fields, including biology, engineering, and medicine. Given the computer vision model matrix A , i.e., the visual representations of concepts, and the language model matrix B , i.e. the language rep-

resentation of the aliases referring to the concepts, we use Procrustes analysis to find the orthogonal matrix Ω that most closely maps A onto B . This problem is equivalent to solving $\min_R \|R - M\|_F$ subject to $R^T R = I$, where $R = UV^T$ can be computed using singular value decomposition. We induce the alignment from a small set of pairs of points, evaluating the alignment on held-out data.

As this requires that the source and target space have the same dimensionality, we use principle component analysis to reduce the dimensions of the larger space whenever a mismatch occurs.

2.4 Evaluation

We induce a linear mapping Ω based on training image-text pairs sampled from A and B , respectively. We then evaluate how close $A\Omega$ is to B by computing retrieval precision on held-out image-text pairs. For example, we could use the mapping of the image of an apple into the word ‘apple’, and the mapping of the image of a banana into the word ‘banana’, as training pairs to induce a mapping Ω . If Ω then maps the image of a lemon onto the word ‘lemon’ as its nearest neighbor³, we say that the precision-at-one (P@1) for this mapping is 100%⁴.

Crucially, instead of populating the target space with just the words from the bimodal dictionary, we populate it with a union of those and another 107,768 words from an English wordlist⁵, filtered to appear at least 5 times in the English Wikipedia and encoded the same way as previously explained. This makes the random retrieval baseline P@1 = $\frac{1}{79059} \approx 0.0013\%$. In practice, our mappings proves to be much more precise, reflecting the structural similarities between language model and computer vision vector spaces.

We evaluate alignment in terms of precision-at- k with $k \in \{1, 10, 100\}$. Note that this performance metric is much more conservative than other metrics used for similar problems, including pairwise matching accuracy, percentile rank, and Pearson correlation (Minnema and Herbelot, 2019). Pairwise matching accuracy and percentile rank have random baseline scores of 0.5, and they converge in the limit. If a has a percentile rank of p in a list \mathcal{A} , it will be higher than a random member

³Here we use CSLS to get the nearest neighbor, see more details in Appendix D.

⁴If two target aliases were listed in the bimodal dictionary for the source image, mapping the image onto either of them would result in P@1=100%.

⁵wordlist-english

of \mathcal{A} p percent of the time. Pearson is monotonically increasing with pairwise matching accuracy, but precision@ k scores are more conservative than any of them for reasonably small values of k . In our case our target space is 79,059 words, and it is possible to have precision@100 values of 100 and still have near-perfect pairwise matching accuracy, percentile rank, and Pearson correlation scores. Precision@ k scores also have the advantage that they are intuitive and practically relevant, e.g., for decoding.

3 Results and Analysis

3.1 Main Results

Our main results for nine VMs and all LMs are presented in Figure 3 (See Appendix E for the remaining VMs). P@1 results, represented by a solid line, far outperform the random baseline of $= \frac{1}{79059}$. Relaxing the search space to 10 neighbors (dashed lines), we see results in the range of 10 to 20 percent, indicating that this percentage of visual concepts were mapped to approximately the right region of the language space, with only a slight deviation. Considering P@100 (dotted line), we observe a further large jump in performance, with close to 70 percent of visual concepts finding a match in the language space when using ResNet, for example. ResNet models score highest overall, followed by SegFormers, while MAE models rank third. We presume that this ranking is the result, in part, of the model’s training objectives: object classification may induce some level of language-informed bias into the ResNet encoder, and similarly for the scene parsing supervision used to train SegFormer models. In this sense, the performance of MAE models, which are fully unsupervised, lands the strongest evidence for the alignability of vision and language spaces—the signal could not come from anywhere else but the intrinsic properties of the visual world encoded by the models.

In Figure 3, we can further study the convergence behavior of VMs and LMs as size grows. The effect of size is clear for MAE models and ResNet models, with precision scores growing from left to right. For SegFormer models, we see an increase in performance from B0 to B3, at which point performance seems to plateau and does not further improve for B5. When it comes to LM size, on the other hand, alignment precision clearly and steadily improves, suggesting that larger models better capture the properties of language.

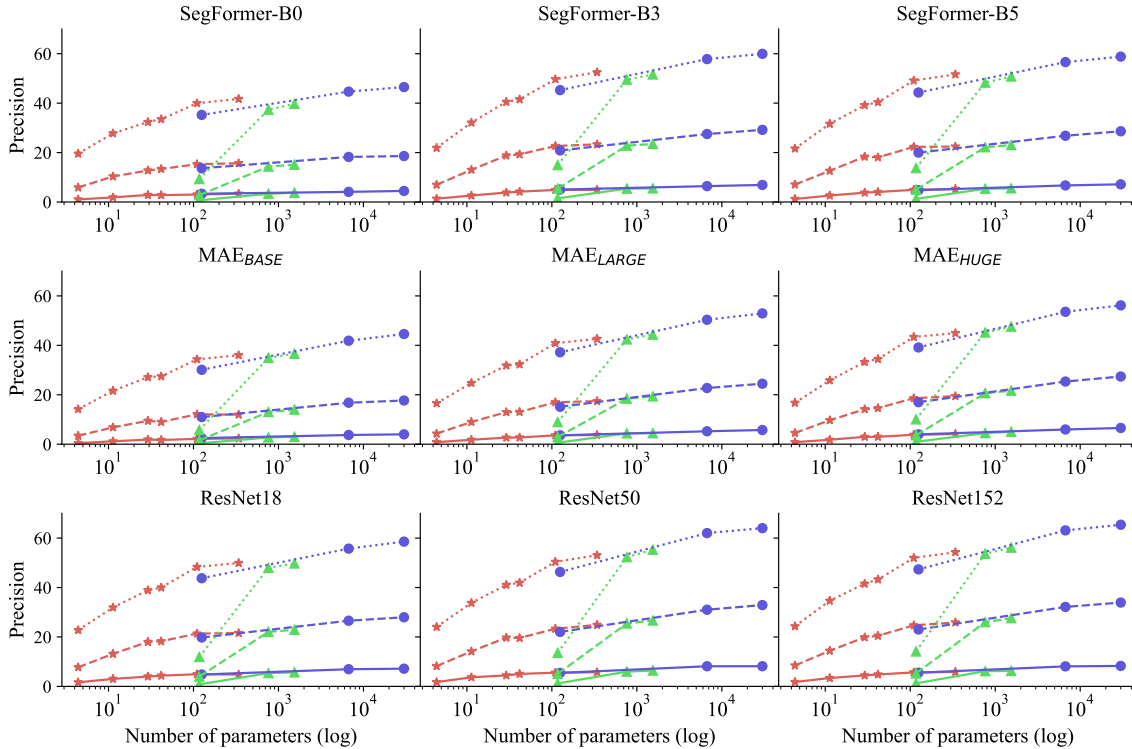


Figure 3: Language models converge toward the geometry of visual models as they grow larger. \star BERT models, \blacktriangle GPT2 models, \bullet OPT models; Dotted line: P@100, dashed line: P@10, solid line: P@1.

With ResNet152 (Figure 3), the best-performing language model, OPT_{30B}, approaches a P@100 of 70%. This means that 7/10 visual concepts are mapped onto a small neighborhood of 100 words—out of total set of 79,059 candidate words—which is quite remarkable. 3/10 images are correctly mapped onto neighborhoods of 10 words, and 1/10, onto exactly the right word. Converge seems log-linear, but with no observed saturation.

Next, we study to what extent alignment precision depends on polysemy and dispersion. In this analysis, we include the largest model per model family for both VMs and LMs.

3.2 Effect of Image Dispersion

We investigate how alignment precision depends on dispersion across the images representing a concept. Image dispersion⁶ is computed by averaging the pair-wise cosine distance between all images associated with a concept (Kielbaso et al., 2015). We split the held-out concepts in the bimodal dictionary in three equally-sized bins based on dispersion and report results in Table 3. Results for ResNet152 suggest that concepts of lower dispersion are easier to align, results for SegFormer-B5 are mixed,

⁶See more details in Appendix B

and results for MAE_{HUGE} follow the exact opposite pattern to ResNet152, with concepts of higher visual dispersion being aligned to the language space with highest precision across all three metrics. We deem these results surprising as intuitively, we expect concepts of lower visual dispersion to have more stable and thus more easily alignable VM representations, regardless of the VM used. The results for MAE_{HUGE} defy this expectation and thus call for further investigation on the effect of visual dispersion. See Table 3 for the full results with ResNet152 and SegFormer-B5, which follow a similar trend.

3.3 Effect of Polysemy

We next investigate the effect of the counterpart to image dispersion in the language space, namely polysemy (the capacity of words to have multiple meanings). Words with multiple meanings may be mapped in positions ‘unexpected’ from the perspective of the non-polysemous visual concept we are mapping onto them, and as such we would expect higher polysemy to cause a drop in precision⁷. To measure this effect, we obtain polysemy counts

⁷Notice that the sentences we obtain from Wikipedia may reflect any of the multiple meanings of a word.

Models	Dispersion	SegFormer-B5			MAE _{HUGE}			ResNet152		
		P@1	P@10	P@100	P@1	P@10	P@100	P@1	P@10	P@100
BERT _L	low	4.3	22.0	52.8	4.3	20.0	46.1	5.8	27.1	58.1
	medium	5.0	22.5	51.1	5.4	23.3	50.1	6.4	27.7	54.4
	high	6.5	22.8	50.9	6.4	28.3	56.5	5.4	22.7	50.2
GPT2 _{XL}	low	5.0	23.3	52.3	5.6	22.5	50.2	6.1	30.4	61.0
	medium	5.1	22.4	50.6	6.5	25.8	53.7	6.7	28.1	57.0
	high	6.5	23.5	49.4	7.6	31.1	57.5	5.9	24.1	50.1
OPT _{30B}	low	6.4	28.8	61.1	7.4	27.0	58.9	7.3	36.6	71.7
	medium	6.9	28.4	58.6	8.4	33.3	62.3	9.5	35.1	64.7
	high	8.2	28.6	56.7	9.9	36.8	66.4	8.1	29.9	59.6

Table 3: Effect of image dispersion. See more results with more models in Appendix E Tables 7, 8, 15.

Models	Polysemy	Pairs	SegF-B5	MAE _{HUGE}	ResNet152	Dispersion	SegF-B5	MAE _{HUGE}	ResNet152
			P@100	P@100	P@100		P@100	P@100	P@100
BERT _L	1	100.8	58.5	60.2	61.7	low	60.4	57.1	61.7
	2-3	178.4	46.4	47.4	49.3	medium	48.3	49.5	52.5
	4+	319.6	37.3	36.5	39.7	high	28.6	28.4	30.7
GPT2 _{XL}	1	100.8	54.6	55.5	58.5	low	43.2	47.6	49.5
	2-3	178.4	52.6	52.7	54.4	medium	49.1	52.2	54.4
	4+	319.6	37.7	40.1	42.5	high	41.1	42.3	45.2
OPT _{30B}	1	100.8	64.3	65.2	68.8	low	60.4	60.0	68.0
	2-3	178.4	56.3	56.9	59.2	medium	56.4	59.9	62.4
	4+	319.6	39.1	41.5	44.7	high	38.6	46.8	44.9

Table 4: Effect of polysemy and language dispersion. See more results with more models in Appendix E Tables 9, 10, 11, 14, 12, and 13.

from BabelNet (Navigli and Ponzetto, 2012) for the aliases in our bimodal dictionary and measure precision over non-polysemous words, words with two or three meanings, and words with four and more meanings. Precision scores for these three bins are presented in Table 4, alongside counts of the image-text pairs located in each bin. Unlike other results reported in the paper, for this table precision is computed separately for each alias, i.e. if a visual concept is associated with 4 aliases and only three of those appear among the nearest 100 neighbors, the P@100 for this concept will be reported as 75%. This is necessary since different aliases for the same concept may land in different bins. The trend, as expected, is for non-polysemous aliases to yield higher precision scores, regardless of VM and LM. For ResNet152 the largest LMs in our experiments, OPT_{30B}, P@100 is 68.8% for the aliases with a single meaning, but only 44.7% for aliases with four or more meanings.

Since many of the aliases in our bimodal dictionary are not covered by BabelNet (in particular, none of the multi-word expressions), we also per-

form an analysis of the ‘language dispersion ⁸’ of embeddings obtained for an aliases in different contexts from Wikipedia—this serves as a proxy to the polysemy of an alias and is measured in the same way as image dispersion. The trend here is similar to the earlier results for BERT and OPT, with low language dispersion resulting in high alignment precision. For GPT2, on the other hand, bin 2-3 yields highest scores: a finding that remains to be explored in the future. The remaining results for all VM and LM combinations can be found in Appendix E Tables 9, 10, 11 and 12.

4 Discussion

Having established that language and vision models converge towards a similar geometry, we discuss the implications of this finding from various practical and theoretical perspectives within AI-related fields and beyond.

⁸See more details in Appendix C

4.1 Implications of Our Findings

Implications for multi-modal AI The idea of cross-modal retrieval is not new (Lazaridou et al., 2014), but previously it has been studied with practical considerations in mind rather than theoretical ones. Recently, Merullo et al. (2022) showed that language representations in LMs are *functionally* equivalent to image representations in VMs, in that a linear transformation applied to an image representation can be used to prompt a language model into producing a relevant caption. We dial back from function and study whether the representations of concepts themselves, on a *fundamental* level, converge toward equivalence (isomorphism). The strong evidence we find in support of this hypothesis indicates that despite the lack of explicit grounding, the representations learned by large pre-trained language models structurally resemble properties of the real, physical world as captured by vision models.

Another related line of work has used image representations as an interlingua for cross-lingual knowledge transfer (Bergsma and Van Durme, 2011; Kiela and Bottou, 2014; Vulić et al., 2016; Hartmann and Søgaard, 2018). What our results suggest is that this is viable, and that the quality of such transfer should increase log-linearly with model size. Previous work did not consider the converge properties of such knowledge transfer.

Implications for the study of emergent properties The literature on large-scale, pretrained models has often discussed seemingly emergent properties (Søgaard et al., 2018; Manning et al., 2020; Garneau et al., 2021; Teehan et al., 2022; Wei et al., 2022), many of which relate to induction of world knowledge. Some have attributed this to memorization, e.g.:

It is also reasonable to assume that more parameters and more training enable better memorization that could be helpful for tasks requiring world knowledge. (Wei et al., 2022)

while others have speculated if this is an effect of compression dynamics (Søgaard et al., 2018; Garneau et al., 2021). The alignability of different modalities can prove to be a very suitable test bed in the study of emergent properties relating to world knowledge. Our experiments above provide initial data points for the study of such properties.

Implications for philosophy Our results have direct implications for two long-standing debates in philosophy: the debate around *strong artificial intelligence* and the so-called *representation wars*.

Searle’s original Chinese Room argument (Searle, 1980) was an attempt to refute the strong artificial intelligence thesis, including that it was possible for a machine to *understand* language. Instead, Searle claims, the interlocutor in his experiment is not endowed with meaning or understanding, but mere symbol manipulation. Here we have showed that an interlocutor endowed only with text converges on inducing the same representational geometry as computer vision models with access to visual impressions of the world. In effect, our experiments show that some level of referential semantics emerges from training on text alone.

The concept of ‘representation wars’ (Williams, 2018) refers to a controversy around the role of representations, especially in doxastic reasoning. The main question is how important mental representations are in such cognitive processes. Cognitive scientists and philosophers aligned with cognitive science represent one view on this, happily postulating discrete, mental representations to explain the observed behavior. Neo-behaviourists, physicalist reductionists, and proponents of embodied cognition have argued to the contrary. To some extent, the positions have softened a bit in recent years. In particular, many in contemporary neuroscience now use the term *representation* just to mean a state of a cognitive system, i.e., neural network, that responds selectively to certain bodily and environmental conditions. This is similar to how the term is used in machine learning. This notion of representation is certainly compatible with neo-behaviorism and physical reductionism. This leaves us with the problem of externalism. Proponents of embodied cognition and other externalists claim that mental representations give us at best a partial story about how meaning is fixed, because meaning depends on external factors. The meaning of a proper name, for example, depends on causal factors relating the name to an initial baptism. We believe that our experiments suggest a way to reconcile this dispute by accounting for how external factors influence our mental representations. This does not answer all concerns externalists may have, but it certainly brings us a lot closer to a reconciliation of this long-standing debate.

Implications for cognitive psychology How representations come about is, as already mentioned, also a problem of neuroscience and cognitive psychology. This literature is rich with inspiration from computational modeling. Cognitive scientists have recently become interested in how self-supervised learning may induce adaptive representations, e.g., Orhan et al. (2020); Halvagal and Zenke (2022). Cognitive scientists have also noted how the objectives of supervised language and vision models bear resemblances to predictive processing (Schrimpf et al., 2018; Caucheteux et al., 2022; Goldstein et al., 2021), but see Antonello and Huth (2022) for a critical discussion of such work. The language models considered here, as well as at least the MAE computer vision models, are unsupervised and have learning objectives that are superficially similar to what is commonly assumed predictive processing. Our results thus lend support to the idea that high-level cognitive functions can be grounded in low-level predictive processing.

5 Conclusion

We have presented a set of experiments specifically targeting the second thought experiment in Bender and Koller (2020). We quantify the degree of isomorphism between the representations of 12 language models and 14 computer vision models, of different sizes, by learning linear maps between them. We do so in order to evaluate whether language and computer vision models learn similar representations of the world, despite being trained on independent data from independent modalities. The evidence for that is overwhelming. In experimental set-ups, where unrelated representations would correspond to precision@ k scores smaller than 0.2%, our linear maps exhibit precision@ k scores of up to 70%. Which is to say that if shown an orange and a banana, Bender and Koller’s octopus would be able to recognize a lemon (with a probability of 70%)—an inferential ability which the authors deem theoretically impossible. More importantly, we see that these scores grow the larger (and better) pretrained models get. Language and computer vision models thus converge on the similar representations the bigger (and better) they get. We discuss the implications of our results for multi-modal artificial intelligence, philosophy, and cognitive psychology. Especially, we argue our results have important implications for philosophi-

cal debates around strong artificial intelligence, the ‘representation wars’, and semantic externalism.

6 Limitations

Our results show that visual concepts can be mapped onto language concepts with high precision when the parameters of the mapping are learned in a supervised fashion. While this experimental setup is sufficient to uncover the structural similarities between visual and language spaces, the argument would be even stronger if we could show that the mapping can be induced in an unsupervised fashion as well, as has been done for cross-lingual embedding spaces (Conneau et al., 2018). We experimented with various algorithms for unsupervised embedding alignment (Conneau et al., 2018; Artetxe et al., 2018; Hoshen and Wolf, 2018) and found that all suffer from the degenerate solution problem described in Hartmann et al. (2018), which is to say that no algorithm is currently available that can effectively map between modalities in an unsupervised fashion. In an investigation of this problem, we experimented with initializing the linear transformation in unsupervised algorithms from that learned with supervised algorithm with an offset, i.e. with various amounts of noise added. We found that the unsupervised algorithms were able to recover from the offset up to a certain point, suggesting that with a sufficiently large number of random restarts, unsupervised mapping should be possible, given that model selection in this case is trivial.

References

- Mostafa Abdou, Artur Kulmizev, Daniel Hershcovich, Stella Frank, Ellie Pavlick, and Anders Søgaard. 2021. [Can language models encode perceptual structure without grounding? a case study in color](#). In *Proceedings of the 25th Conference on Computational Natural Language Learning*, pages 109–132. Online. Association for Computational Linguistics.
- Richard Antonello and Alexander Huth. 2022. [Predictive Coding or Just Feature Discovery? An Alternative Account of Why Language Models Fit Brain Data](#). *Neurobiology of Language*, pages 1–16.
- Mikel Artetxe, Gorka Labaka, and Eneko Agirre. 2018. [A robust self-learning method for fully unsupervised cross-lingual mappings of word embeddings](#). In *ACL*.
- Jason Baumgartner, Savvas Zannettou, Brian Keegan, Megan Squire, and Jeremy Blackburn. 2020. [The pushshift reddit dataset](#). *CoRR*, abs/2001.08435.

- Emily M. Bender and Alexander Koller. 2020. [Climbing towards NLU: On meaning, form, and understanding in the age of data](#). In *Proceedings of the 58th Annual Meeting of the Association for Computational Linguistics*, pages 5185–5198, Online. Association for Computational Linguistics.
- Shane Bergsma and Benjamin Van Durme. 2011. Learning bilingual lexicons using the visual similarity of labeled web images. In *Proceedings of the Twenty-Second International Joint Conference on Artificial Intelligence - Volume Volume Three, IJ-CAI'11*, page 1764–1769. AAAI Press.
- Caucheteux C and Jean-Rémi King. 2022. Brains and algorithms partially converge in natural language processing. *Communications biology*.
- Charlotte Caucheteux, Alexandre Gramfort, and Jean-Rémi King. 2022. [Long-range and hierarchical language predictions in brains and algorithms](#). *Nature Human Behaviour*, abs/2111.14232.
- Alexis Conneau, Guillaume Lample, Marc’Aurelio Ranzato, Ludovic Denoyer, and Hervé Jégou. 2018. [Word Translation Without Parallel Data](#). In *Proceedings of ICLR 2018*.
- Jacob Devlin, Ming-Wei Chang, Kenton Lee, and Kristina Toutanova. 2019. [BERT: Pre-training of deep bidirectional transformers for language understanding](#). In *Proceedings of the 2019 Conference of the North American Chapter of the Association for Computational Linguistics: Human Language Technologies, Volume 1 (Long and Short Papers)*, pages 4171–4186, Minneapolis, Minnesota. Association for Computational Linguistics.
- Leo Gao, Stella Biderman, Sid Black, Laurence Golding, Travis Hoppe, Charles Foster, Jason Phang, Horace He, Anish Thite, Noa Nabeshima, Shawn Presser, and Connor Leahy. 2021. [The pile: An 800gb dataset of diverse text for language modeling](#). *CoRR*, abs/2101.00027.
- Nicolas Garneau, Mareike Hartmann, Anders Sandholm, Sebastian Ruder, Ivan Vulic, and Anders Søgaard. 2021. [Analogy training multilingual encoders](#). *Proceedings of the AAAI Conference on Artificial Intelligence*, 35(14):12884–12892.
- Ariel Goldstein, Zaid Zada, Eliav Buchnik, Mariano Schain, Amy Price, Bobbi Aubrey, Samuel A. Nastase, Amir Feder, Dotan Emanuel, Alon Cohen, Aren Jansen, Harshvardhan Gazula, Gina Choe, Aditi Rao, Se Catherine Kim, Colton Casto, Lora Fanda, Werner Doyle, Daniel Friedman, Patricia Dugan, Lucia Melloni, Roi Reichart, Sasha Devore, Adeen Flinker, Liat Hasenfratz, Omer Levy, Avinatan Hassidim, Michael Brenner, Yossi Matias, Kenneth A. Norman, Orrin Devinsky, and Uri Hasson. 2021. [Thinking ahead: spontaneous prediction in context as a keystone of language in humans and machines](#). *bioRxiv*.
- Manu Srinath Halvagal and Friedemann Zenke. 2022. [The combination of hebbian and predictive plasticity learns invariant object representations in deep sensory networks](#). *bioRxiv*.
- Stevan Harnad. 2007. The symbol grounding problem. *Scholarpedia*, 2(7):2373.
- Mareike Hartmann, Yova Kementchedjheva, and Anders Søgaard. 2018. [Why is unsupervised alignment of English embeddings from different algorithms so hard?](#) In *Proceedings of the 2018 Conference on Empirical Methods in Natural Language Processing*, pages 582–586, Brussels, Belgium. Association for Computational Linguistics.
- Mareike Hartmann and Anders Søgaard. 2018. [Limitations of cross-lingual learning from image search](#). In *Proceedings of The Third Workshop on Representation Learning for NLP*, pages 159–163, Melbourne, Australia. Association for Computational Linguistics.
- Kaiming He, Xinlei Chen, Saining Xie, Yanghao Li, Piotr Dollár, and Ross Girshick. 2022. Masked autoencoders are scalable vision learners. In *Proceedings of the IEEE/CVF Conference on Computer Vision and Pattern Recognition*, pages 16000–16009.
- Kaiming He, Xiangyu Zhang, Shaoqing Ren, and Jian Sun. 2016. [Deep Residual Learning for Image Recognition](#). In *Proceedings of 2016 IEEE Conference on Computer Vision and Pattern Recognition, CVPR '16*, pages 770–778. IEEE.
- Yedid Hoshen and Lior Wolf. 2018. An iterative closest point method for unsupervised word translation. In *CoRR*, page 1801.06126.
- Douwe Kiela and Léon Bottou. 2014. [Learning image embeddings using convolutional neural networks for improved multi-modal semantics](#). In *Proceedings of the 2014 Conference on Empirical Methods in Natural Language Processing (EMNLP)*, pages 36–45, Doha, Qatar. Association for Computational Linguistics.
- Douwe Kiela, Ivan Vulić, and Stephen Clark. 2015. [Visual bilingual lexicon induction with transferred ConvNet features](#). In *Proceedings of the 2015 Conference on Empirical Methods in Natural Language Processing*, pages 148–158, Lisbon, Portugal. Association for Computational Linguistics.
- Angeliki Lazaridou, Elia Bruni, and Marco Baroni. 2014. [Is this a wampimuk? cross-modal mapping between distributional semantics and the visual world](#). In *Proceedings of the 52nd Annual Meeting of the Association for Computational Linguistics (Volume 1: Long Papers)*, pages 1403–1414, Baltimore, Maryland. Association for Computational Linguistics.
- Yinhan Liu, Myle Ott, Naman Goyal, Jingfei Du, Mandar Joshi, Danqi Chen, Omer Levy, Mike Lewis, Luke Zettlemoyer, and Veselin Stoyanov. 2019.

- Roberta: A robustly optimized BERT pretraining approach. *CoRR*, abs/1907.11692.
- Paul Lodge and Marc Bobro. 1998. [Stepping back inside leibniz’s mill](#). *The Monist*, 81(4):553–572.
- Christopher D. Manning, Kevin Clark, John Hewitt, Urvashi Khandelwal, and Omer Levy. 2020. [Emergent linguistic structure in artificial neural networks trained by self-supervision](#). *Proceedings of the National Academy of Sciences*, 117(48):30046–30054.
- Jack Merullo, Louis Castricato, Carsten Eickhoff, and Ellie Pavlick. 2022. [Linearly mapping from image to text space](#).
- Gosse Minnema and Aurélie Herbelot. 2019. [From brain space to distributional space: The perilous journeys of fMRI decoding](#). In *Proceedings of the 57th Annual Meeting of the Association for Computational Linguistics: Student Research Workshop*, pages 155–161, Florence, Italy. Association for Computational Linguistics.
- Roberto Navigli and Simone Paolo Ponzetto. 2012. [Babelnet: The automatic construction, evaluation and application of a wide-coverage multilingual semantic network](#). *Artif. Intell.*, 193:217–250.
- Emin Orhan, Vaibhav Gupta, and Brenden M Lake. 2020. [Self-supervised learning through the eyes of a child](#). In *Advances in Neural Information Processing Systems*, volume 33, pages 9960–9971. Curran Associates, Inc.
- Adam Paszke, Sam Gross, Francisco Massa, Adam Lerer, James Bradbury, Gregory Chanan, Trevor Killeen, Zeming Lin, Natalia Gimelshein, Luca Antiga, Alban Desmaison, Andreas Kopf, Edward Yang, Zachary DeVito, Martin Raison, Alykhan Tejani, Sasank Chilamkurthy, Benoit Steiner, Lu Fang, Junjie Bai, and Soumith Chintala. 2019. [Pytorch: An imperative style, high-performance deep learning library](#). In *Advances in Neural Information Processing Systems 32*, pages 8024–8035. Curran Associates, Inc.
- Steven T. Piantadosi and Felix Hill. 2022. [Meaning without reference in large language models](#).
- Alec Radford, Jeff Wu, Rewon Child, David Luan, Dario Amodei, and Ilya Sutskever. 2019. [Language models are unsupervised multitask learners](#).
- Miloš Radovanović, Alexandros Nanopoulos, and Mirjana Ivanović. 2010. [Hubs in space: Popular nearest neighbors in high-dimensional data](#). *J. Mach. Learn. Res.*, 11:2487–2531.
- Stephen Roller, Emily Dinan, Naman Goyal, Da Ju, Mary Williamson, Yinhan Liu, Jing Xu, Myle Ott, Eric Michael Smith, Y-Lan Boureau, and Jason Weston. 2021. [Recipes for building an open-domain chatbot](#). In *Proceedings of the 16th Conference of the European Chapter of the Association for Computational Linguistics: Main Volume*, pages 300–325, Online. Association for Computational Linguistics.
- Olga Russakovsky, Jia Deng, Hao Su, Jonathan Krause, Sanjeev Satheesh, Sean Ma, Zhiheng Huang, Andrej Karpathy, Aditya Khosla, Michael Bernstein, Alexander C. Berg, and Li Fei-Fei. 2015. [ImageNet Large Scale Visual Recognition Challenge](#). *International Journal of Computer Vision (IJCV)*, 115(3):211–252.
- Magnus Sahlgren and Fredrik Carlsson. 2021. [The singleton fallacy: Why current critiques of language models miss the point](#). *Frontiers in Artificial Intelligence*, 4(682578).
- Peter H Schönemann. 1966. [A generalized solution of the orthogonal procrustes problem](#). *Psychometrika*, 31(1):1–10.
- Martin Schrimpf, Jonas Kubilius, Ha Hong, Najib Majaj, Rishi Rajalingham, Elias B. Issa, Kohitij Kar, Pouya Bashivan, Jonathan Prescott-Roy, Kailyn Schmidt, Daniel L. K. Yamins, and James J. DiCarlo. 2018. [Brain-score: Which artificial neural network for object recognition is most brain-like?](#) *bioRxiv*.
- John R. Searle. 1980. [Minds, brains, and programs](#). *Behavioral and Brain Sciences*, 3:417–424.
- Anders Søgaard, Sebastian Ruder, and Ivan Vulić. 2018. [On the Limitations of Unsupervised Bilingual Dictionary Induction](#). In *Proceedings of ACL 2018*.
- Ryan Teehan, Miruna Clinciu, Oleg Serikov, Eliza Szczechla, Natasha Seelam, Shachar Mirkin, and Aaron Gokaslan. 2022. [Emergent structures and training dynamics in large language models](#). In *Proceedings of BigScience Episode #5 – Workshop on Challenges & Perspectives in Creating Large Language Models*, pages 146–159, virtual+Dublin. Association for Computational Linguistics.
- Trieu H. Trinh and Quoc V. Le. 2018. [A simple method for commonsense reasoning](#). *ArXiv*, abs/1806.02847.
- Iulia Turc, Ming-Wei Chang, Kenton Lee, and Kristina Toutanova. 2019. [Well-read students learn better: On the importance of pre-training compact models](#). *arXiv preprint arXiv:1908.08962v2*.
- Ivan Vulić, Douwe Kiela, Stephen Clark, and Marie-Francine Moens. 2016. [Multi-modal representations for improved bilingual lexicon learning](#). In *Proceedings of the 54th Annual Meeting of the Association for Computational Linguistics (Volume 2: Short Papers)*, pages 188–194, Berlin, Germany. Association for Computational Linguistics.
- Jason Wei, Yi Tay, Rishi Bommasani, Colin Raffel, Barret Zoph, Sebastian Borgeaud, Dani Yogatama, Maarten Bosma, Denny Zhou, Donald Metzler, Ed H. Chi, Tatsunori Hashimoto, Oriol Vinyals, Percy Liang, Jeff Dean, and William Fedus. 2022. [Emergent abilities of large language models](#). *Transactions on Machine Learning Research*. Survey Certification.

Daniel Williams. 2018. [Predictive processing and the representation wars](#). *Minds and Machines*, 28(1):141–172.

Thomas Wolf, Lysandre Debut, Victor Sanh, Julien Chaumond, Clement Delangue, Anthony Moi, Pierric Cistac, Tim Rault, Remi Louf, Morgan Funtowicz, Joe Davison, Sam Shleifer, Patrick von Platen, Clara Ma, Yacine Jernite, Julien Plu, Canwen Xu, Teven Le Scao, Sylvain Gugger, Mariama Drame, Quentin Lhoest, and Alexander Rush. 2020. [Transformers: State-of-the-art natural language processing](#). In *Proceedings of the 2020 Conference on Empirical Methods in Natural Language Processing: System Demonstrations*, pages 38–45, Online. Association for Computational Linguistics.

Enze Xie, Wenhai Wang, Zhiding Yu, Anima Anandkumar, Jose M. Alvarez, and Ping Luo. 2021. [Segmenter: Simple and efficient design for semantic segmentation with transformers](#). In *Advances in Neural Information Processing Systems*, volume 34, pages 12077–12090. Curran Associates, Inc.

Susan Zhang, Stephen Roller, Naman Goyal, Mikel Artetxe, Moya Chen, Shuohui Chen, Christopher Dewan, Mona Diab, Xian Li, Xi Victoria Lin, Todor Mihaylov, Myle Ott, Sam Shleifer, Kurt Shuster, Daniel Simig, Punit Singh Koura, Anjali Sridhar, Tianlu Wang, and Luke Zettlemoyer. 2022. [Opt: Open pre-trained transformer language models](#).

Bolei Zhou, Hang Zhao, Xavier Puig, Sanja Fidler, Adela Barriuso, and Antonio Torralba. 2017. Scene parsing through ade20k dataset. *computer vision and pattern recognition*.

Yukun Zhu, Ryan Kiros, Richard S. Zemel, Ruslan Salakhutdinov, Raquel Urtasun, Antonio Torralba, and Sanja Fidler. 2015. Aligning books and movies: Towards story-like visual explanations by watching movies and reading books. *2015 IEEE International Conference on Computer Vision (ICCV)*, pages 19–27.

A Reproducibility

Our code are openly available at [IPLVEs].

Implementation Our implementation is based on PyTorch v.1.12.0 (Paszke et al., 2019) and Transformer v4.25.1 (Wolf et al., 2020) for Python 3.9.13 and builds on code from the repositories in Table 5 and 6.

LMs	Links
BERT _{TINY}	https://huggingface.co/google/bert_uncased_L-2_H-128_A-2
BERT _{MINI}	https://huggingface.co/google/bert_uncased_L-4_H-256_A-4
BERT _{SMALL}	https://huggingface.co/google/bert_uncased_L-4_H-512_A-8
BERT _{MEDIUM}	https://huggingface.co/google/bert_uncased_L-8_H-512_A-8
BERT _{BASE}	https://huggingface.co/bert-base-uncased
BERT _{LARGE}	https://huggingface.co/bert-large-uncased
GPT2 _{BASE}	https://huggingface.co/gpt2
GPT2 _{LARGE}	https://huggingface.co/gpt2-large
GPT2 _{XL}	https://huggingface.co/gpt2-xl
OPT _{125M}	https://huggingface.co/facebook/opt-125m
OPT _{6.7B}	https://huggingface.co/facebook/opt-6.7b
OPT _{30B}	https://huggingface.co/facebook/opt-30b

Table 5: Links of 12 Transformer-based language models used in our experiments.

VMs	Links
SegFormer-B0	https://huggingface.co/nvidia/segformer-b0-finetuned-ade-512-512
SegFormer-B1	https://huggingface.co/nvidia/segformer-b1-finetuned-ade-512-512
SegFormer-B2	https://huggingface.co/nvidia/segformer-b2-finetuned-ade-512-512
SegFormer-B3	https://huggingface.co/nvidia/segformer-b3-finetuned-ade-512-512
SegFormer-B4	https://huggingface.co/nvidia/segformer-b4-finetuned-ade-512-512
SegFormer-B5	https://huggingface.co/nvidia/segformer-b5-finetuned-ade-640-640
MAE _{BASE}	https://huggingface.co/facebook/vit-mae-base
MAE _{LARGE}	https://huggingface.co/facebook/vit-mae-large
MAE _{HUGE}	https://huggingface.co/facebook/vit-mae-huge
ResNet18	https://pypi.org/project/img2vec-pytorch/
ResNet34	
ResNet50	
ResNet101	
ResNet152	

Table 6: Links of 14 computer vision models used in our experiments.

B Image Dispersion

The image dispersion d of a concept alias a is defined as the average pairwise cosine distance between all the image representations i_1, i_2, \dots, i_n in the set of n images for a given alias (Kielbaso et al., 2015):

$$d(a) = \frac{2}{n(n-1)} \sum_{k < j \leq n} 1 - \frac{i_j \cdot i_k}{|i_j| |i_k|}$$

C Language Dispersion

The language dispersion d of a concept alias a is defined as the average pairwise cosine distance between all the corresponding word representations w_1, w_2, \dots, w_n in the set of n sentences for a given alias:

$$d(a) = \frac{2}{n(n-1)} \sum_{k < j \leq n} 1 - \frac{w_j \cdot w_k}{|w_j| |w_k|}$$

D Cross-domain Similarity Local Scaling (CSLS)

Nearest neighbors are naturally asymmetric, which means if y is a K -NN of x , it does not follow that x is also a K -NN of y . In high-dimensional spaces (Radovanović et al., 2010), the nearest neighbor rule can lead to a phenomenon called hubness, where some vectors (hubs) are nearest neighbors of many other points, while others (anti-hubs) are not nearest neighbors of any point. This is detrimental to matching pairs based on the nearest neighbor rule. To address this issue, Conneau et al. (2018) propose a bi-partite neighborhood graph, in which each word of a given dictionary is connected to its K nearest neighbors in the other language. The neighborhood of a mapped source word embedding Wx_s , denoted as $N_T(Wx_s)$, is represented on the bipartite graph. It consists of K elements, all of which are words from the target language. Similarly, the neighborhood of a target word t , denoted as $N_S(y_t)$. The mean similarity between a source embedding x_s and its corresponding target neighborhood is considered as

$$r_T(Wx_s) = \frac{1}{K} \sum_{y_t \in N_T(Wx_s)} \cos(Wx_s, y_t),$$

where $\cos(\dots)$ means cosine similarity. They use $r_S(y_t)$ to represent the mean similarity of a target word y_t to its neighborhood. The definition of Cross-domain Similarity Local Scaling (CSLS) between mapped source words and target words is

$$CSLS(Wx_s, y_t) = 2\cos(Wx_s, y_t) - r_T(Wx_s) - r_S(y_t).$$

Instead of using this for two language domains, we use this method for our vision and English words domain.

E More Results

Figure 4 shows the P@k results of aligning SegFormer (B1, B2, and B4) and ResNet (34 and 101) to all LMs.

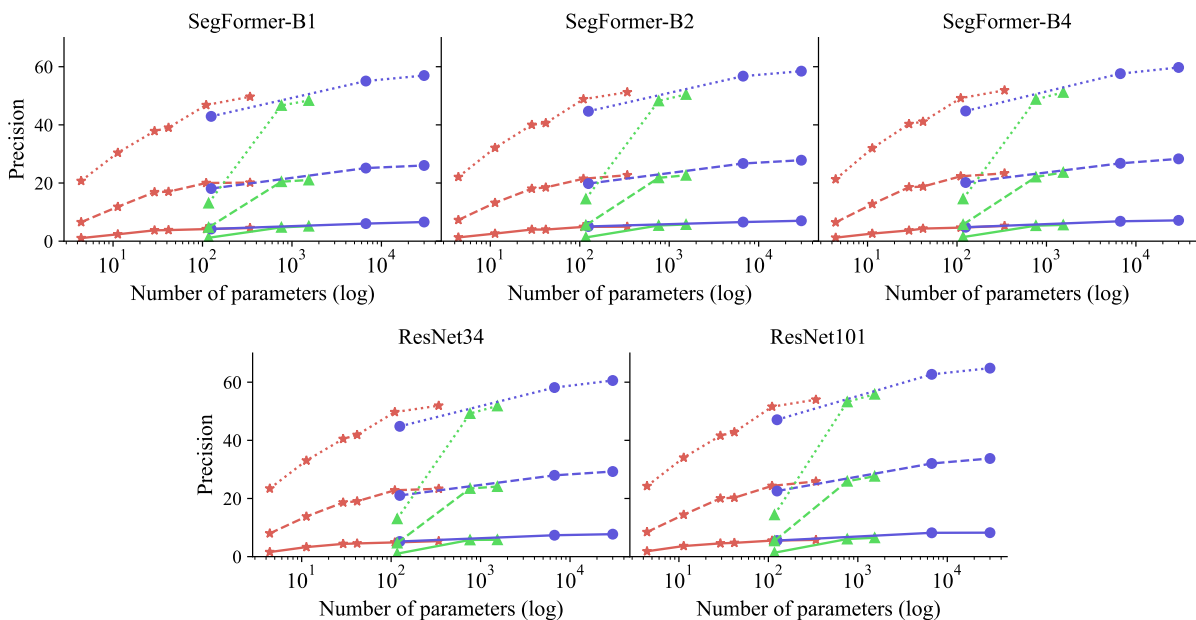


Figure 4: Language models converge toward the geometry of remaining visual models as they grow larger. \star BERT models, \blacktriangle GPT2 models, \bullet OPT models; Dotted line: P@100, dashed line: P@10, solid line: P@1.

Models	Disp.	P@1	P@10	P@100
BERT _{TINY}	low	1.84	10.09	27.11
	med.	1.94	8.46	24.84
	high	1.55	6.75	20.87
BERT _{MINI}	low	3.63	16.49	37.62
	med.	3.20	14.28	35.13
	high	3.32	12.39	31.12
BERT _{SMALL}	low	4.11	22.47	45.17
	med.	4.59	20.06	41.96
	high	4.65	16.89	37.32
BERT _{MEDIUM}	low	4.63	23.20	46.80
	med.	5.33	20.55	43.65
	high	4.53	17.54	39.11
BERT _{BASE}	low	6.05	26.76	55.73
	med.	5.96	26.17	52.55
	high	4.92	21.06	47.53
BERT _{LARGE}	low	5.81	27.07	58.12
	med.	6.35	27.73	54.44
	high	5.37	22.73	50.16
GPT2 _{BASE}	low	1.17	6.02	15.76
	med.	1.41	5.68	14.90
	high	1.08	3.92	11.63
GPT2 _{LARGE}	low	6.04	28.87	57.58
	med.	6.53	26.49	54.63
	high	5.91	22.54	48.56
GPT2 _{XL}	low	6.14	30.38	60.98
	med.	6.71	28.14	57.03
	high	5.92	24.12	50.14
OPT _{125M}	low	5.19	25.19	50.07
	med.	5.75	23.32	48.00
	high	5.70	20.43	43.79
OPT _{6.7B}	low	7.29	35.02	69.46
	med.	8.82	33.19	62.46
	high	8.22	28.13	57.18
OPT _{30B}	low	7.29	36.61	71.71
	med.	9.46	35.11	64.65
	high	8.11	29.94	59.62

Table 7: Image dispersion experiments based on ResNet152 and various LMs.

Models	Disp.	P@1	P@10	P@100
BERT _{TINY}	low	1.02	8.10	24.35
	med.	1.18	6.46	19.93
	high	1.54	6.58	20.58
BERT _{MINI}	low	2.14	13.55	33.61
	med.	2.86	12.32	30.578
	high	2.83	11.96	30.69
BERT _{SMALL}	low	3.37	19.94	41.22
	med.	3.50	17.60	38.45
	high	4.52	17.43	37.76
BERT _{MEDIUM}	low	4.22	19.39	42.04
	med.	3.73	18.16	39.63
	high	4.20	16.58	39.38
BERT _{BASE}	low	4.35	22.78	50.57
	med.	4.68	22.14	48.86
	high	5.77	21.92	48.01
BERT _{LARGE}	low	4.29	21.97	52.83
	med.	5.02	22.49	51.12
	high	6.53	22.83	50.89
GPT2 _{BASE}	low	1.23	4.74	13.29
	med.	1.36	4.92	13.86
	high	1.18	5.30	14.02
GPT2 _{LARGE}	low	4.94	22.72	48.59
	med.	5.05	21.47	49.24
	high	6.11	22.30	47.00
GPT2 _{XL}	low	4.98	23.31	52.32
	med.	5.06	22.42	50.56
	high	6.54	23.49	49.43
OPT _{125M}	low	4.17	20.81	43.78
	med.	4.29	19.62	44.70
	high	5.89	19.47	44.42
OPT _{6.7B}	low	5.55	26.95	58.67
	med.	6.88	26.78	56.40
	high	7.71	26.63	54.67
OPT _{30B}	low	6.35	28.83	61.12
	med.	6.91	28.43	58.62
	high	8.21	28.61	56.67

Table 8: Image dispersion experiments based on SegFormer-B5 and various LMs.

Models	Disp.	P@10	P@100
ResNet18	low	25.40	56.61
	med.	19.26	48.50
	high	8.34	26.82
ResNet34	low	27.34	59.53
	med.	21.19	50.04
	high	9.26	28.26
ResNet50	low	28.98	60.13
	med.	23.14	51.41
	high	9.64	29.71
ResNet101	low	30.21	61.60
	med.	24.05	52.21
	high	10.14	30.17
ResNet152	low	30.43	61.71
	med.	23.94	52.52
	high	10.03	30.66
SegFormer-B0	low	17.77	47.03
	med.	14.88	40.60
	high	5.52	21.79
SegFormer-B1	low	23.61	56.27
	med.	18.33	47.70
	high	7.43	27.18
SegFormer-B2	low	26.98	59.35
	med.	20.58	48.61
	high	8.41	27.82
SegFormer-B3	low	28.00	61.10
	med.	20.48	49.94
	high	9.02	29.09
SegFormer-B4	low	27.73	60.55
	med.	20.76	48.57
	high	8.92	28.67
SegFormer-B5	low	27.28	60.44
	med.	20.14	48.31
	high	8.13	28.59
MAE _{BASE}	low	11.27	35.71
	med.	14.81	40.37
	high	10.75	31.47
MAE _{LARGE}	low	15.62	42.72
	med.	20.65	46.48
	high	16.26	38.40
MAE _{HUGE}	low	27.43	57.09
	med.	21.74	49.48
	high	9.64	28.39

Table 9: Language dispersion experiments based on BERT_{LARGE} and various VMs.

Models	Disp.	P@10	P@100
ResNet18	low	15.76	42.83
	med.	22.70	48.12
	high	18.10	39.54
ResNet34	low	16.49	44.63
	med.	23.62	50.04
	high	19.09	41.73
ResNet50	low	18.49	49.04
	med.	25.95	53.27
	high	21.34	44.32
ResNet101	low	19.40	49.24
	med.	27.00	54.22
	high	21.79	45.18
ResNet152	low	19.64	49.46
	med.	26.75	54.44
	high	22.01	45.21
SegFormer-B0	low	10.30	33.12
	med.	14.85	38.56
	high	11.36	30.50
SegFormer-B1	low	14.57	41.38
	med.	20.78	47.28
	high	16.53	38.12
SegFormer-B2	low	15.33	42.99
	med.	23.33	48.94
	high	17.43	40.35
SegFormer-B3	low	16.04	44.02
	med.	23.22	49.88
	high	18.67	42.26
SegFormer-B4	low	16.77	43.94
	med.	22.52	49.26
	high	18.75	40.95
SegFormer-B5	low	16.52	43.19
	med.	22.05	49.13
	high	18.53	41.09
MAE _{BASE}	low	11.78	36.27
	med.	16.74	40.83
	high	13.10	32.25
MAE _{LARGE}	low	16.88	44.30
	med.	22.69	49.09
	high	18.21	39.15
MAE _{HUGE}	low	19.15	47.65
	med.	25.51	52.23
	high	20.12	42.27

Table 10: Language dispersion experiments based on GPT2_{XL} and various VMs.

Models	Disp.	P@10	P@100
ResNet18	low	25.44	60.17
	med.	26.46	56.44
	high	16.45	37.53
ResNet34	low	26.42	62.23
	med.	28.12	57.80
	high	17.20	40.06
ResNet50	low	30.71	66.88
	med.	30.84	60.85
	high	19.76	42.95
ResNet101	low	32.03	67.33
	med.	31.42	61.88
	high	20.25	44.07
ResNet152	low	32.16	67.95
	med.	31.64	62.36
	high	20.25	44.92
SegFormer-B0	low	17.32	48.27
	med.	17.74	44.52
	high	9.41	28.02
SegFormer-B1	low	23.69	58.87
	med.	25.19	54.49
	high	14.60	36.61
SegFormer-B2	low	24.74	60.72
	med.	27.36	55.68
	high	15.98	38.16
SegFormer-B3	low	25.97	60.91
	med.	28.59	57.49
	high	17.41	40.07
SegFormer-B4	low	25.00	61.28
	med.	27.42	57.16
	high	16.74	39.53
SegFormer-B5	low	26.25	60.43
	med.	27.77	56.43
	high	16.49	38.58
MAE _{BASE}	low	18.03	49.10
	med.	20.73	47.68
	high	13.81	35.05
MAE _{LARGE}	low	24.01	57.00
	med.	28.68	56.29
	high	20.13	43.82
MAE _{HUGE}	low	27.46	60.02
	med.	31.22	59.94
	high	22.92	46.80

Table 11: Language dispersion experiments based on OPT_{30B} and various VMs.

Models	Meanings	Pairs	P@10	P@100
BERT _{TINY}	1	100.8	8.98	28.66
	2&3	178.4	9.90	26.13
	4+	319.6	8.76	22.50
BERT _{MINI}	1	100.8	17.30	41.23
	2&3	178.4	15.07	36.89
	4+	319.6	15.29	34.89
BERT _{SMALL}	1	100.8	18.25	47.13
	2&3	178.4	19.22	40.54
	4+	319.6	18.89	37.46
BERT _{MEDIUM}	1	100.8	19.08	49.30
	2&3	178.4	19.19	41.79
	4+	319.6	17.15	37.21
BERT _{BASE}	1	100.8	23.68	58.16
	2&3	178.4	22.57	47.34
	4+	319.6	17.89	36.41
BERT _{LARGE}	1	100.8	22.55	58.49
	2&3	178.4	20.23	46.36
	4+	319.6	17.06	37.26
GPT2 _{BASE}	1	100.8	5.73	16.66
	2&3	178.4	6.35	15.59
	4+	319.6	4.81	13.91
GPT2 _{LARGE}	1	100.8	23.95	54.45
	2&3	178.4	27.84	50.50
	4+	319.6	19.00	37.45
GPT2 _{XL}	1	100.8	26.18	54.62
	2&3	178.4	27.04	52.58
	4+	319.6	18.52	37.70
OPT _{125M}	1	100.8	22.96	53.77
	2&3	178.4	27.11	49.13
	4+	319.6	19.91	37.81
OPT _{6.7B}	1	100.8	31.45	62.34
	2&3	178.4	29.49	53.68
	4+	319.6	20.56	38.72
OPT _{30B}	1	100.8	32.94	64.32
	2&3	178.4	29.93	56.25
	4+	319.6	20.15	39.06

Table 12: Polysemy experiments with SegFormer-B5 and various LMs.

Models	Meanings	Pairs	P@10	P@100
BERT _{TINY}	1	100.8	9.17	29.70
	2&3	178.4	8.72	24.21
	4+	319.6	6.70	19.81
BERT _{MINI}	1	100.8	15.84	40.70
	2&3	178.4	16.04	34.74
	4+	319.6	14.26	31.99
BERT _{SMALL}	1	100.8	18.47	46.07
	2&3	178.4	20.31	40.59
	4+	319.6	18.38	36.15
BERT _{MEDIUM}	1	100.8	21.57	51.19
	2&3	178.4	19.10	41.92
	4+	319.6	17.80	35.63
BERT _{BASE}	1	100.8	22.61	59.34
	2&3	178.4	21.89	48.42
	4+	319.6	18.82	36.95
BERT _{LARGE}	1	100.8	23.61	60.19
	2&3	178.4	21.27	47.37
	4+	319.6	19.03	36.51
GPT2 _{BASE}	1	100.8	6.73	14.95
	2&3	178.4	7.05	16.00
	4+	319.6	3.85	9.84
GPT2 _{LARGE}	1	100.8	23.19	55.48
	2&3	178.4	28.46	52.73
	4+	319.6	23.62	40.11
GPT2 _{XL}	1	100.8	25.31	57.61
	2&3	178.4	29.23	53.52
	4+	319.6	23.32	40.12
OPT _{125M}	1	100.8	23.67	50.96
	2&3	178.4	26.21	48.98
	4+	319.6	21.11	38.78
OPT _{6.7B}	1	100.8	31.39	63.23
	2&3	178.4	31.64	55.51
	4+	319.6	24.11	41.31
OPT _{30B}	1	100.8	34.25	65.17
	2&3	178.4	32.31	56.87
	4+	319.6	25.31	41.53

Table 13: Polysemy experiments with MAE_{HUGE} and various LMs.

Models	Meanings	Pairs	P@10	P@100
BERT _{TINY}	1	100.8	11.22	32.44
	2&3	178.4	10.73	29.61
	4+	319.6	10.32	25.06
BERT _{MINI}	1	100.8	17.41	44.86
	2&3	178.4	18.02	40.26
	4+	319.6	17.13	36.73
BERT _{SMALL}	1	100.8	20.25	51.23
	2&3	178.4	20.77	44.40
	4+	319.6	20.44	39.71
BERT _{MEDIUM}	1	100.8	23.95	52.92
	2&3	178.4	20.12	45.72
	4+	319.6	19.42	39.53
BERT _{BASE}	1	100.8	27.29	62.01
	2&3	178.4	21.91	50.40
	4+	319.6	19.73	39.10
BERT _{LARGE}	1	100.8	27.03	61.66
	2&3	178.4	22.91	49.31
	4+	319.6	19.38	39.70
GPT2 _{BASE}	1	100.8	6.42	13.94
	2&3	178.4	8.36	17.99
	4+	319.6	5.53	12.91
GPT2 _{LARGE}	1	100.8	26.98	57.10
	2&3	178.4	30.21	54.06
	4+	319.6	24.14	42.53
GPT2 _{XL}	1	100.8	28.10	58.45
	2&3	178.4	29.87	54.37
	4+	319.6	24.83	42.52
OPT _{125M}	1	100.8	26.59	56.49
	2&3	178.4	26.62	52.34
	4+	319.6	23.63	41.25
OPT _{6.7B}	1	100.8	33.59	66.26
	2&3	178.4	32.71	57.38
	4+	319.6	25.05	44.28
OPT _{30B}	1	100.8	35.47	68.80
	2&3	178.4	33.83	59.22
	4+	319.6	25.04	44.73

Table 14: Polysemy experiments with ResNet152 and various LMs.

Models	Disp.	P@1	P@10	P@100
BERT _{TINY}	low	1.33	5.46	19.35
	med.	1.09	6.07	19.15
	high	1.39	7.02	22.62
BERT _{MINI}	low	1.95	10.44	28.28
	med.	2.28	12.14	29.23
	high	3.33	14.92	34.39
BERT _{SMALL}	low	3.06	15.12	35.96
	med.	3.54	17.50	36.75
	high	5.09	20.89	42.88
BERT _{MEDIUM}	low	3.65	15.80	37.45
	med.	3.72	17.39	38.40
	high	4.66	21.63	43.85
BERT _{BASE}	low	4.58	20.16	46.16
	med.	3.86	22.35	47.42
	high	6.24	26.07	54.24
BERT _{LARGE}	low	4.34	19.98	46.14
	med.	5.37	23.34	50.11
	high	6.41	28.25	56.54
GPT2 _{BASE}	low	1.01	4.13	12.60
	med.	0.98	4.04	11.88
	high	1.76	5.84	13.44
GPT2 _{LARGE}	low	5.08	20.80	47.31
	med.	5.87	24.95	50.87
	high	6.91	30.29	56.17
GPT2 _{XL}	low	5.56	22.49	50.18
	med.	6.46	25.81	53.71
	high	7.64	31.11	57.46
OPT _{125M}	low	4.06	17.68	41.08
	med.	5.27	20.59	44.41
	high	6.23	24.91	49.88
OPT _{6.7B}	low	6.36	27.15	56.47
	med.	7.86	30.49	59.02
	high	9.00	35.02	64.08
OPT _{30B}	low	7.37	28.96	58.88
	med.	8.40	33.34	62.27
	high	9.93	36.78	66.38

Table 15: Image dispersion experiments based on MAE_{HUGE} and various LMs.